International Journal of Engineering Research & Technology (IJERT)
ISSN: 2278-0181
Vol. 9 Issue 03, March-2020

Pier Thickness Influence for Turbulent Water Flow using Particle Image Velocimetry

Jose Elias Villa Herrera[a], Cornelio Alvarez Herrera[a], Jose Guadalupe Murillo Ramirez[b], Humberto Silva Hidalgo[a], Jose Luis Herrera Aguilar[a], Antonio Campa Rodriguez[a]
a, Universidad Autónoma de Chihuahua, Facultad de Ingeniería, Nuevo Campus Universitario, Circuito Universitario S/N, C.P, Chihuahua, Chih., México.
b, Centro de Investigación en Materiales Avanzados S. C., Miguel de Cervantes 120, Complejo Industrial Chihuahua. C.P, México.

***Abstract*:- The obstruction of water flow by structural elements such as the bridge pier generates turbulence, which fosters the phenomenon of local scour, especially during rain seasons over extraordinary avenues, and sediment drag presence is bigger. The non-destructive full-field optical technique, commonly called particle image velocimetry, has been a resource of great importance in providing a better understanding of fluid movement, in which data about its turbulence is obtained. With this technology, within a hydraulic scale channel, it was possible to observe the water flow that passed through a circular pier, using three thicknesses, obtaining images of its behavior and figuring a nomogram about turbulence distance.**

Keywords: Thickness; Pier; Flow; Scour; Particles; Image; Velocimetry.

INTRODUCTION

Particle Image Velocimetry (PIV) since the early 1980s [6], is an optical non-destructive full-field technique, it has been used as a resource of great importance to study the behaviour of water movement over surfaces. With the PIV and software for image processing [1], data movement of water has been obtained from vectors in turbulence locations that are generated at the bottom of a channel by obstruction structures such as bridge piers. Figure 1, it is shown PIV equipment and hydraulic channel.

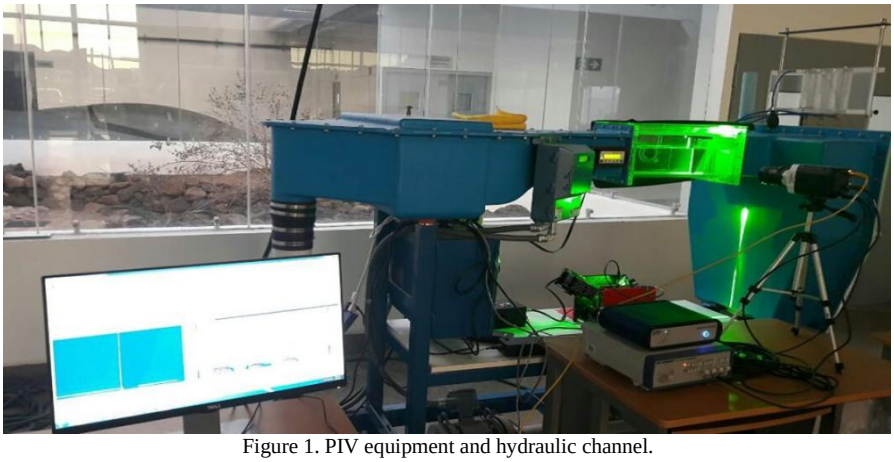

Figure 1. PIV equipment and hydraulic channel.

Since computers and cameras with CCD technology (Charge Coupled Device) were developed, it laid the foundations of this digital technology [2], giving rise to high-resolution imaging [7], which is intended to deepen the understanding of the phenomenon of scour, characterizing the flow speed, its hydrodynamics, linear patterns, vorticity and shear stress [3; 5]. It is also possible to analyse the size of the sediment transportation and the depth of scour that can be generated around structures such as a bridge pier [14].

PIER SCOUR

The formation of pits around the bridge pier over a river or channel, is almost inevitable, generating scour that reduces the bottom bed due to a high level of turbulence and vorticity [9]. The presence of foundations on the river bed should be avoided as much as possible [10] and, if necessary, be as slender as possible in order to avoid its obstruction as much as possible [11].

(This work is licensed under a Creative Commons Attribution 4.0 International License.)

International Journal of Engineering Research & Technology (IJERT)
ISSN: 2278-0181
Vol. 9 Issue 03, March-2020

Nowadays, results are not completely satisfactory to face the problem of scour, so studies such as the placement of sensors could help to understand in greater detail the water flow behaviour, which generates the removal of sediments around the foundation of bridges piers and abutments. These same studies are used to verify the structural quality of the bridge using vibration methods [4], which is expected to improve the available deterministic stochastic or empirical mathematical models. It is hoped the combination of many studies, will lead to laboratory results that are more attached to the real system, and that numerical models - whether simple or very complex - that are used to characterize sediment erosion, offer better understanding of scour in the future [12]. With this, scour problems in the pier of a bridge such as shown in Figure 2, could be foreseen coming from the original design, or resolved after being evidenced in existing infrastructure.

Figure 2. Light scour on a bridge pier after raining.

METHODS

A video of the water flow in a 0.50 m long, 0.15 m deep and 0.15 m width, hydraulic channel with a 1.5HP electric pump, was captured in the laboratory using a CCD camera previously calibrated, in order to characterize the movement when obstructed by three thickness scale circular pier model. Tracer and reflective 9-13µm particles inside water were used for illumination by a 532 nanometer green laser [13]. Subsequently, the video was loaded and processed using a visualization software, in order to extract data from it. PIV, is based on the study of speed through mathematical expression, $\boldsymbol{V = d / t}$, where $\boldsymbol{d}$ is the distance travelled by a particle at a given time $\boldsymbol{t}$. That's way **V** is the speed acquired by the particles when taking the trajectories of the flow.

The displacement is obtained using a Gaussian function at the peak of the correlation, and finding the exact maximum location [8]. Figure 3, it is shown a CCD camera, laser and hydraulic channel laser illuminated. Figure 4, Additional photos are shown for CCD camera and 532 nanometer green laser equipment.

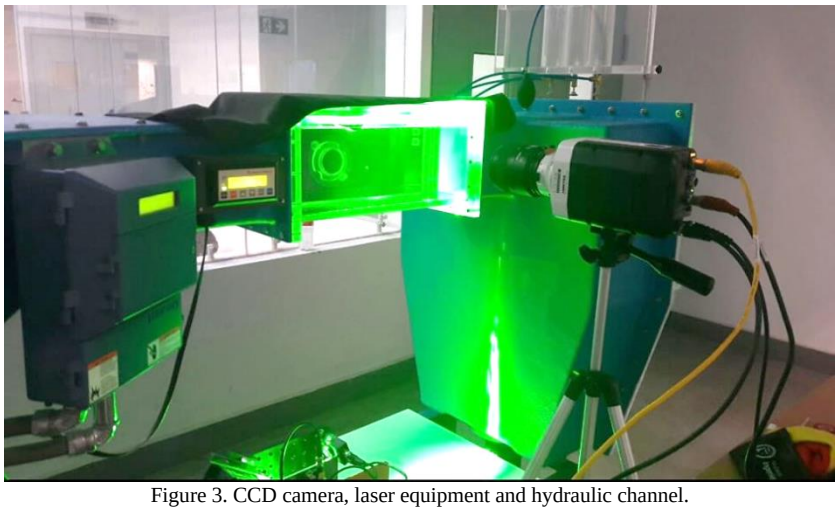

Figure 3. CCD camera, laser equipment and hydraulic channel.

(This work is licensed under a Creative Commons Attribution 4.0 International License.)

International Journal of Engineering Research & Technology (IJERT)
ISSN: 2278-0181
Vol. 9 Issue 03, March-2020

Figure 4. CCD camera and 532 nanometer green laser equipment.

For this experiment, subsequently a water 0.09 m flow level, was applied with particles seeded and illuminated by the laser beam, with a speed of 0.0084 m / s, equivalent to a flow rate of 0.107253 l/s, for upstream area, observing downflow position, with a Reynolds number (Re) = 235.87, then it was decided to increase speed for turbulence appreciation up to 0.117 m / s, equivalent to a flow rate of 1.577 l/s, with a Reynolds number (Re) = 3289 and 0.163 m/s, equivalent to a flow rate of 2.22 l/s, with a Reynolds number (Re)= 4573 for downstream area, creating a vorticity distance nomogram. (500≤Re≤2000) $\boldsymbol{Re = \rho v R/\mu}$, where: $\boldsymbol{\rho}$ = water density; $\boldsymbol{v}$ = water speed; $\boldsymbol{R}$ =hydraulic radius and $\boldsymbol{\mu}$ =water dynamic viscosity. In Figure 3 it is shown this experiment with the laser-lit particles and Figure 5, it is shown the location of the upstream and downstream areas.

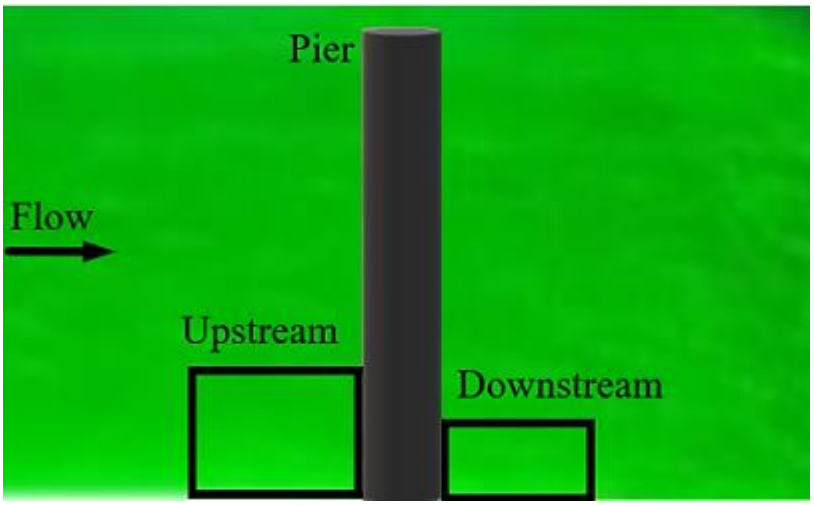

Figure 5. Location of the upstream and downstream areas is shown.

Finally, the video was recorded with a CCD camera, taking 40 images of 24 x 24 pixels at 700 microseconds. The videos were processed by LaVision DaVis 8 software, from which data were obtained in DAT - System format. The files in DAT - System format, were post-processed by the TecPlot - 360 software to obtain images, which final result was the average of the 40 of them formed in video. It is shown Figure 6, pier model and illuminated flow particles with pier by laser. It is shown in Figure 7, pier model and high speed downflow illustration at upstream location area arrowed by red line.

(This work is licensed under a Creative Commons Attribution 4.0 International License.)

International Journal of Engineering Research & Technology (IJERT)
ISSN: 2278-0181
Vol. 9 Issue 03, March-2020

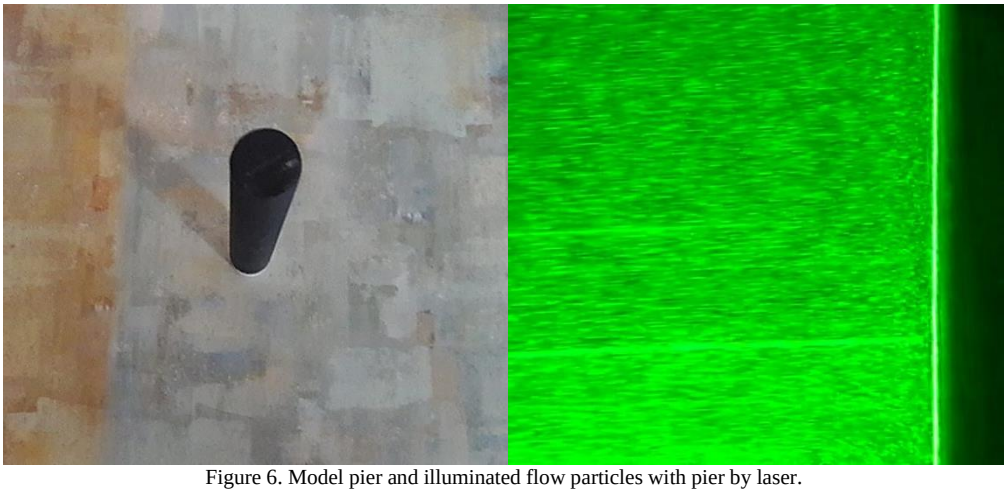

Figure 6. Model pier and illuminated flow particles with pier by laser.

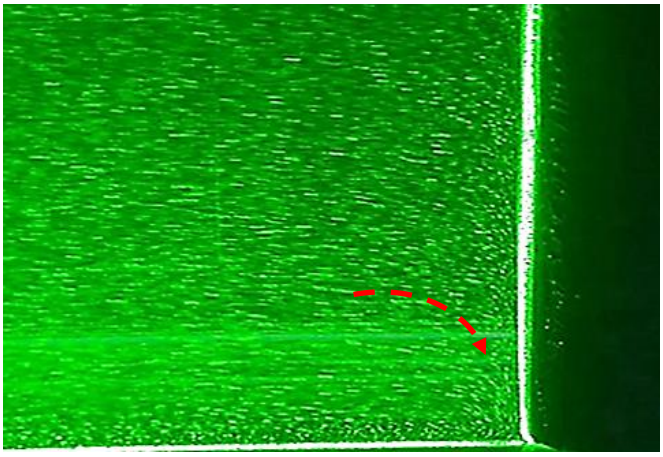

Figure 7. Pier model and high speed downflow illustration at upstream location area.

RESULTS

In Figures 8, 9 and 10, at 0.0084 m/s for upstream section, the obstructed water flow behaviour was shown by circular scale pier model, using 10, 20 and 30 mm thicknesses, vortex was appreciated at different positions due to the pier's thickness, going further back water downflow and upper. Hence, for downstream the turbulence was bigger, from slender pier to thicker pier, until hitting against it. Arrowed line leads each horizontal and vertical distance from vortex to pier, indicating their position.

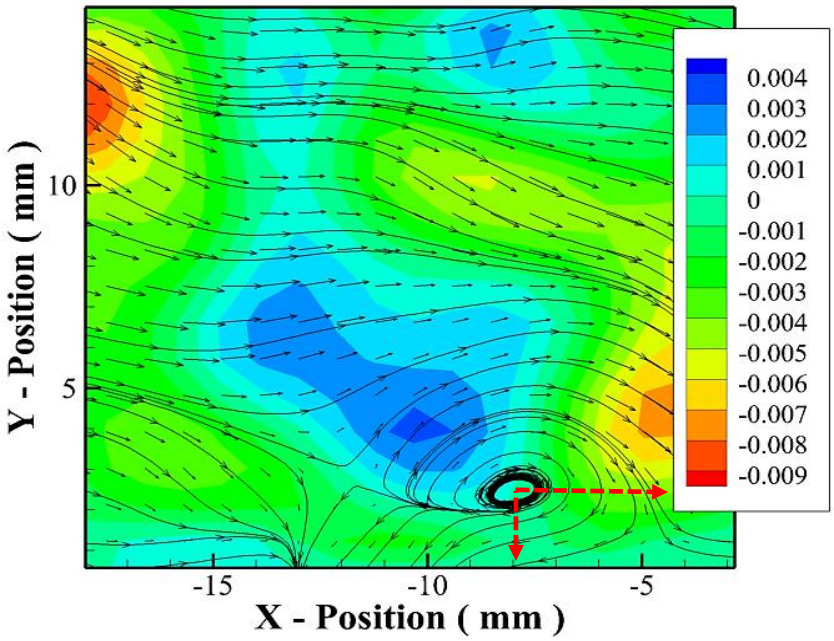

Figure 8. Upstream 10 mm pier (7.9;2.6) vortex coordinates.

(This work is licensed under a Creative Commons Attribution 4.0 International License.)

International Journal of Engineering Research & Technology (IJERT)
ISSN: 2278-0181
Vol. 9 Issue 03, March-2020

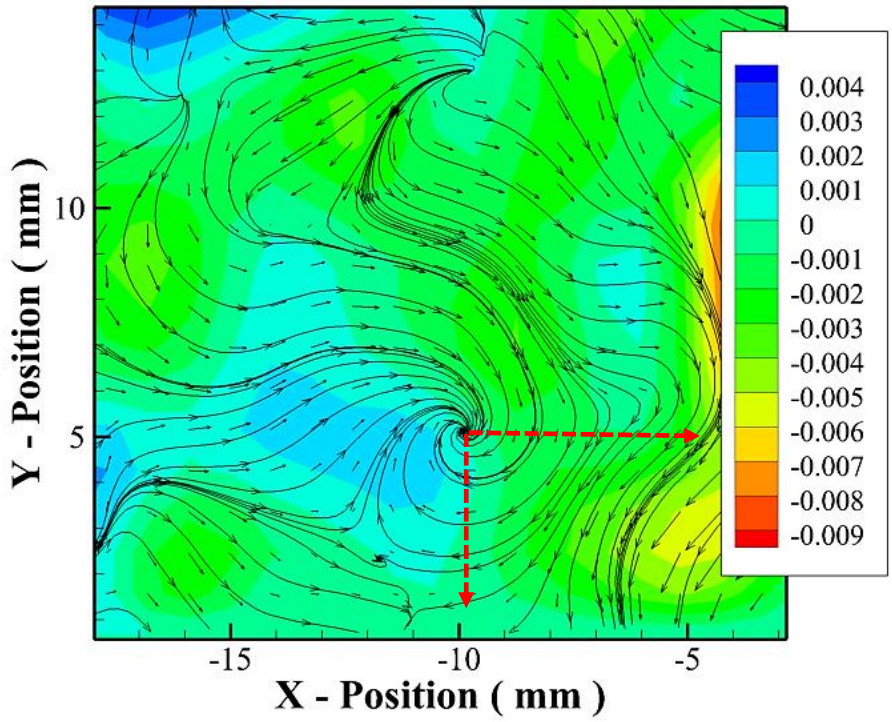

Figure 9. Upstream 20 mm pier (9.9;5.1) vortex coordinates.

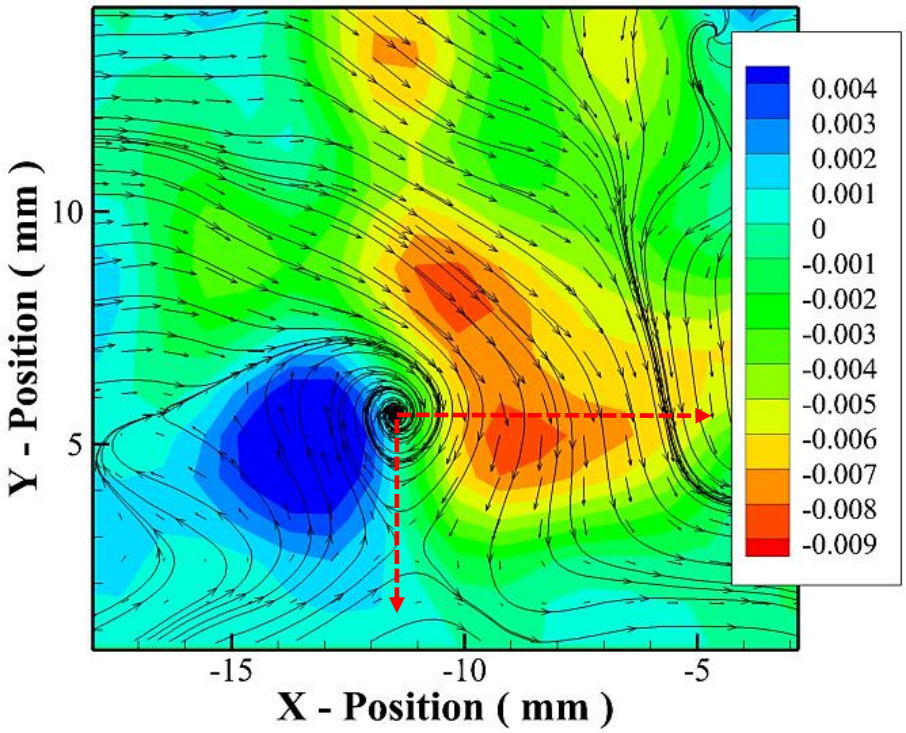

Figure 10. Upstream 30 mm pier (11.5;5.7) vortex coordinates.

(This work is licensed under a Creative Commons Attribution 4.0 International License.)

International Journal of Engineering Research & Technology (IJERT)
ISSN: 2278-0181
Vol. 9 Issue 03, March-2020

It is shown in table1, down flow vortex and its position due to pier thickness.
(500⩽Re⩽2000)

Pier (mm)	Speed (m/s)	(Re)	X – Position (mm)	Y – Position (mm)
10	0.0084	235.87	7.90	2.60
20	0.0084	235.87	9.90	5.10
30	0.0084	235.87	11.50	5.70

Table 1. Vortex position in X and Y axis.

It is shown in Figure 11, the three vortex positions at the same time due to the pier obstruction, using a blue circle for the slimmer one and grey polygon for thicker one.

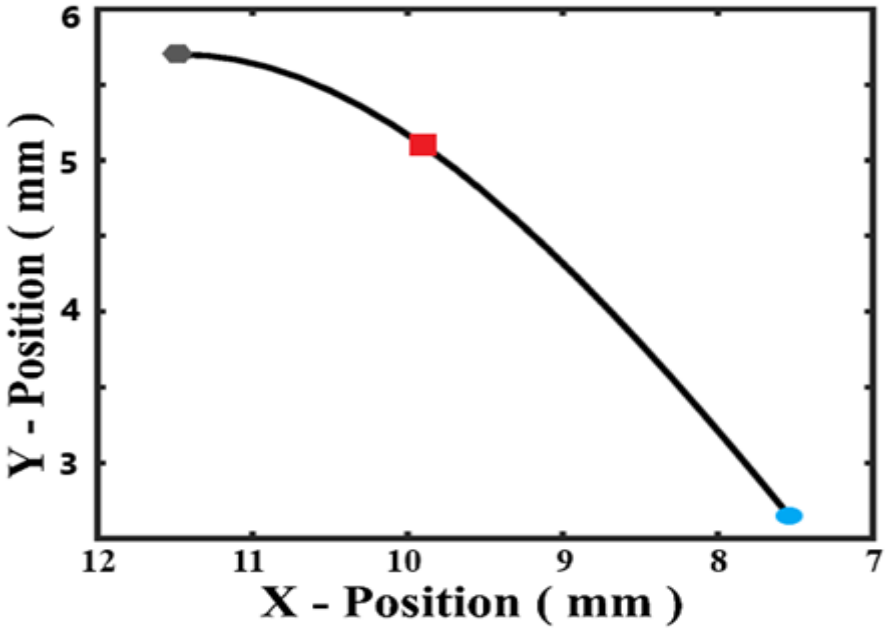

Figure 11. Three vortex positions at the same time due to the pier obstruction.

In Figure 12, it can be seen the percentage of distance downflow vortex relation, from each other from pier upstream area. The blue color represents 10 mm pier with 27%, red color represents 20 mm pier with 34% and grey color represents 30 mm pier with 39%. Therefore, it means there is a 12% difference from slender pier to thicker pier due to the obstruction.

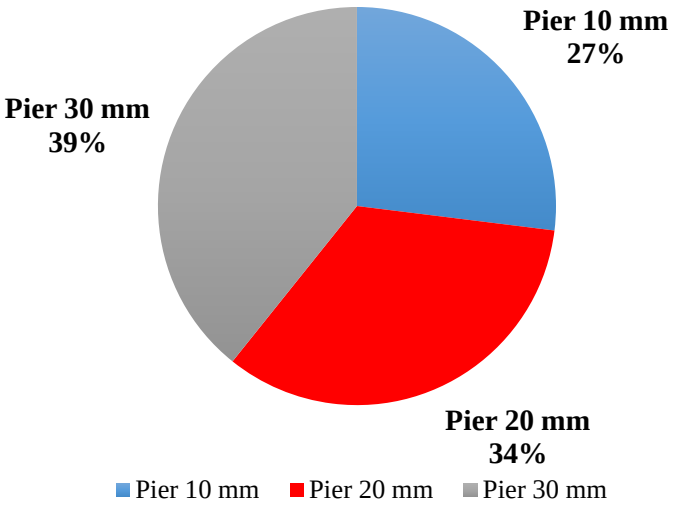

Figure 12. Percentage about distance down flow vortex relation.

(This work is licensed under a Creative Commons Attribution 4.0 International License.)

International Journal of Engineering Research & Technology (IJERT)
ISSN: 2278-0181
Vol. 9 Issue 03, March-2020

It is shown for Figure 13, 14 and 15 at 0.117 m/s speed then Figure16, 17 and 18 at 0.163 m/s speed corresponding to downstream area, how flow water vorticity was generated due to the different pier thickness, started from hitting the bottom up to be next the pier. Arrowed line leads each horizontal distance from vortex to pier. It is shown in Figure 19, a top 20 mm pier view accomplishing observe the Von Karman vortices at 0.117 m / s speed.

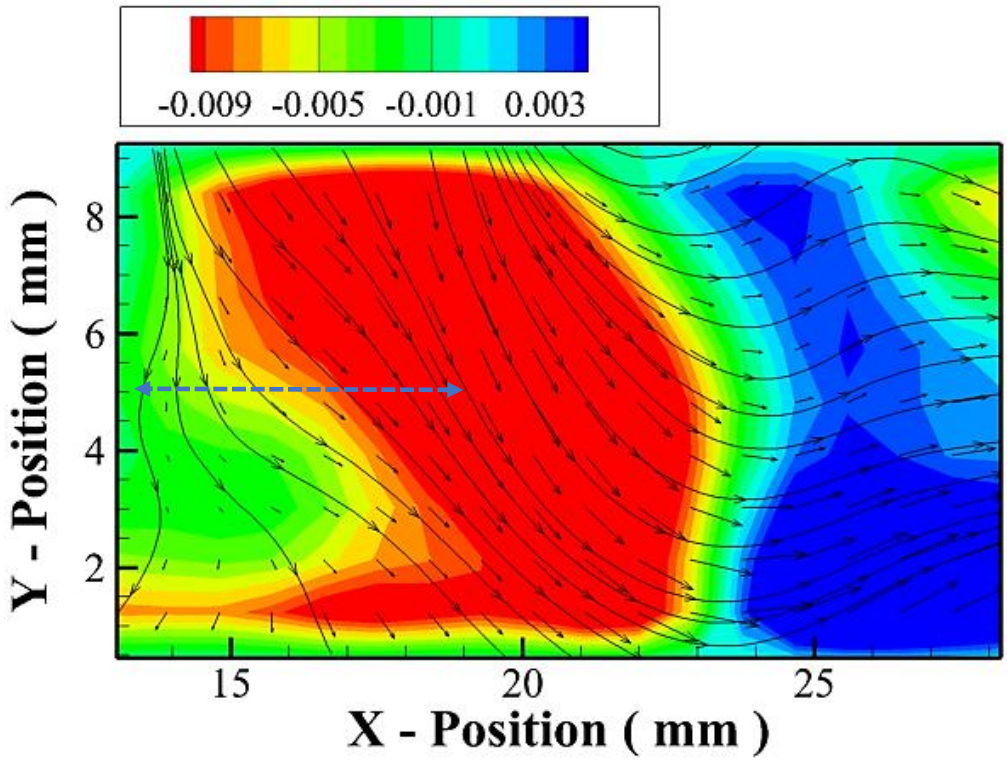

Figure 13. Downstream 10 mm pier (6.0 mm) horizontal distance from water hitting the bottom.

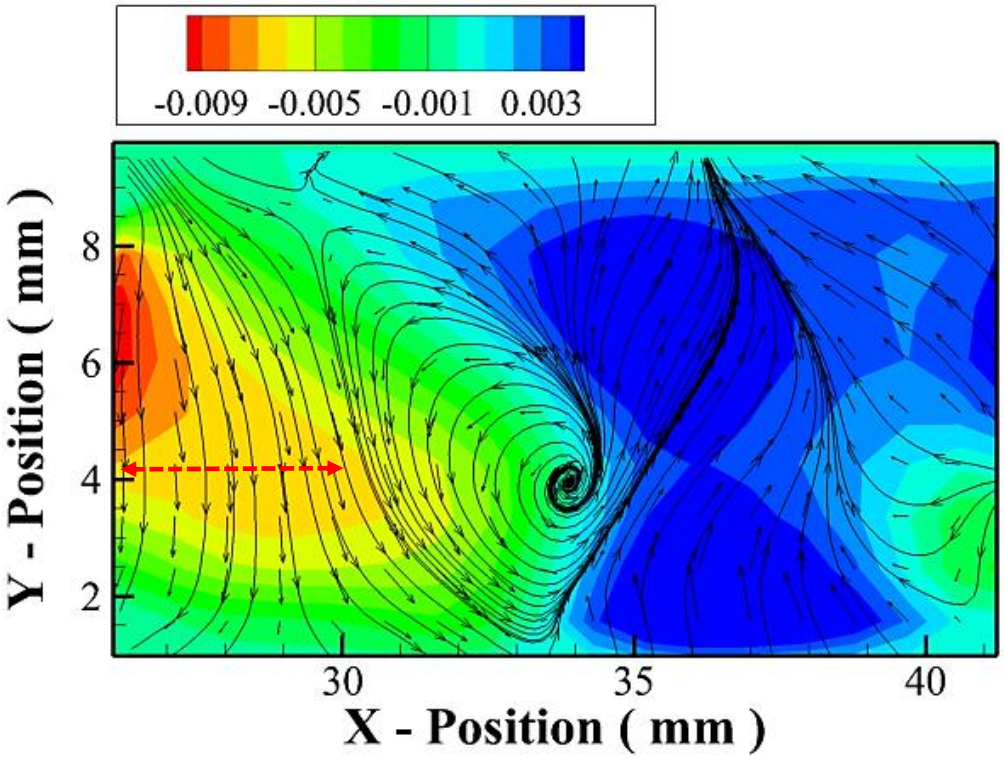

Figure 14. Downstream 20 mm pier (4.0 mm) horizontal distance from vortex water hitting the bottom.

(This work is licensed under a Creative Commons Attribution 4.0 International License.)

International Journal of Engineering Research & Technology (IJERT)
ISSN: 2278-0181
Vol. 9 Issue 03, March-2020

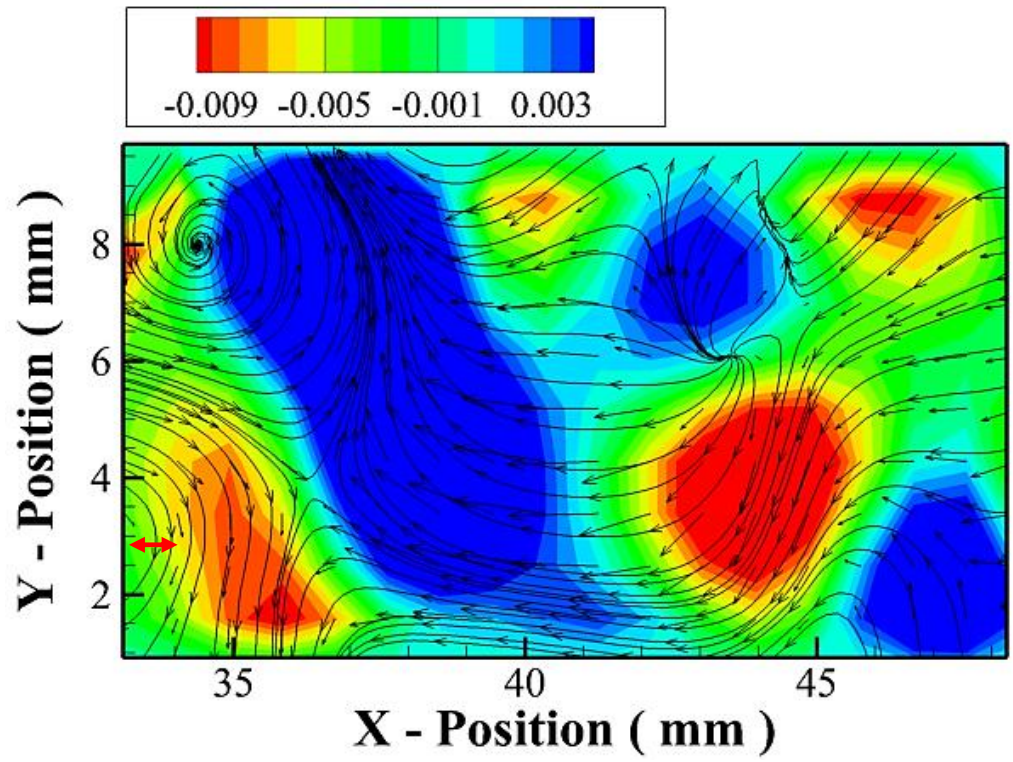

Figure 15. Downstream 30 mm pier (1.0 mm) horizontal distance from vortex water hitting the bottom next to pier.

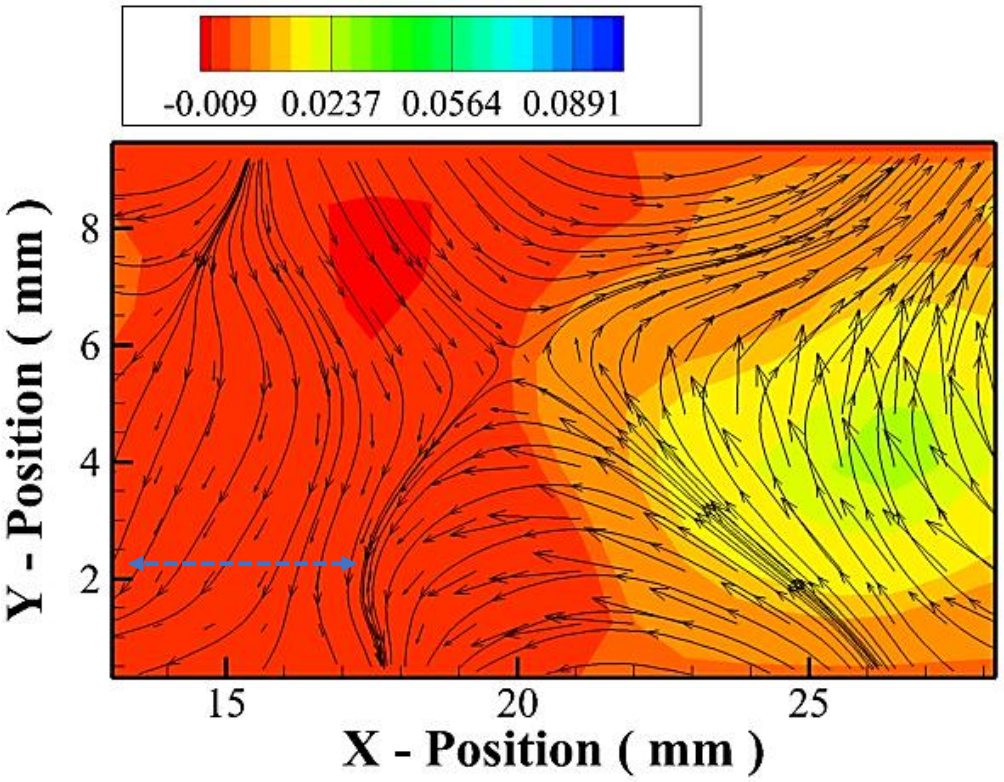

Figure 16. Downstream 10 mm pier (4.5 mm) horizontal distance from water hitting the bottom.

(This work is licensed under a Creative Commons Attribution 4.0 International License.)

International Journal of Engineering Research & Technology (IJERT)
ISSN: 2278-0181
Vol. 9 Issue 03, March-2020

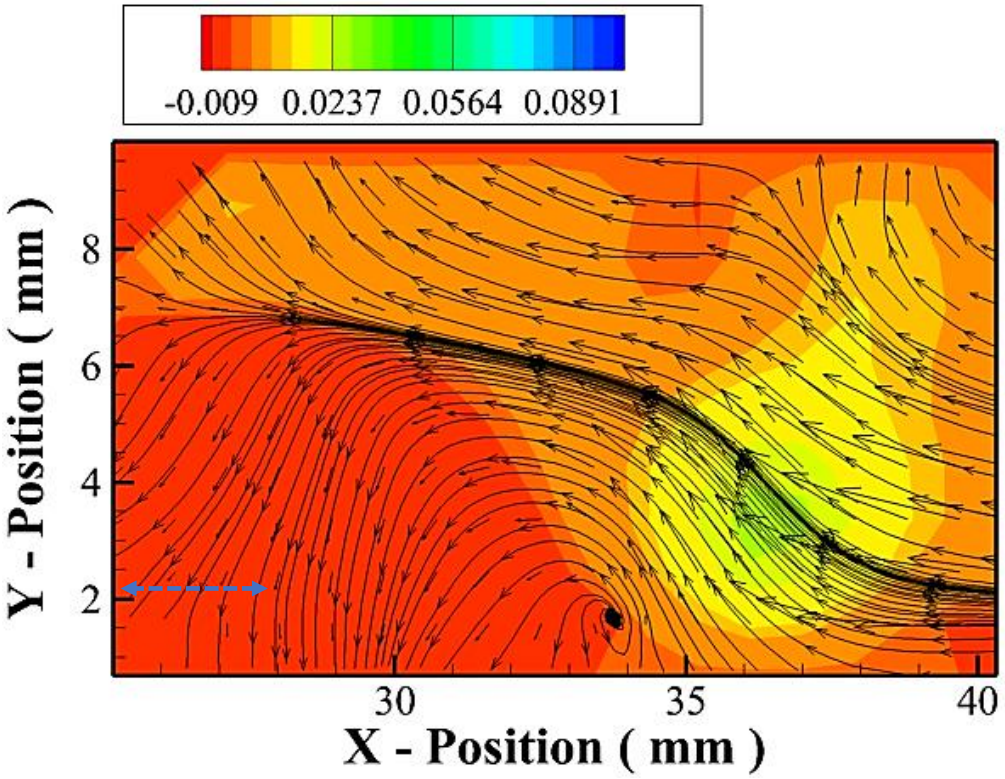

Figure 17. Downstream 20 mm pier (2.5 mm) horizontal distance from vortex water hitting the bottom.

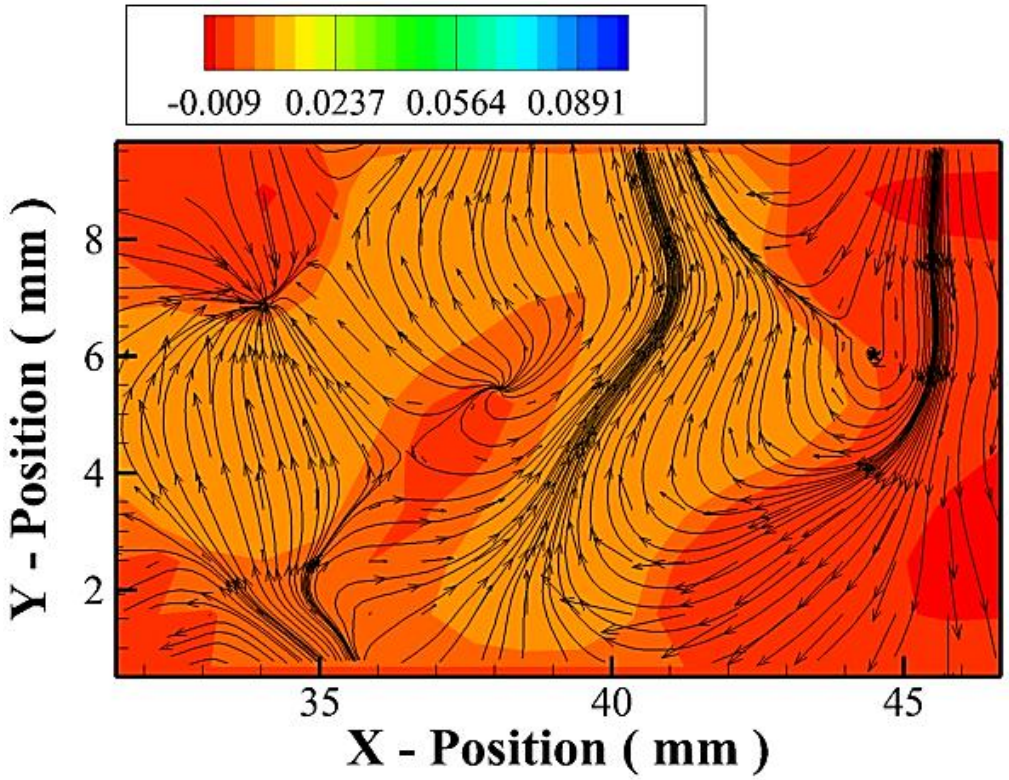

Figure 18. Downstream 30 mm pier (0.0 mm) horizontal distance from multiple vortices water hitting completely the bottom to pier.

(This work is licensed under a Creative Commons Attribution 4.0 International License.)

International Journal of Engineering Research & Technology (IJERT)
ISSN: 2278-0181
Vol. 9 Issue 03, March-2020

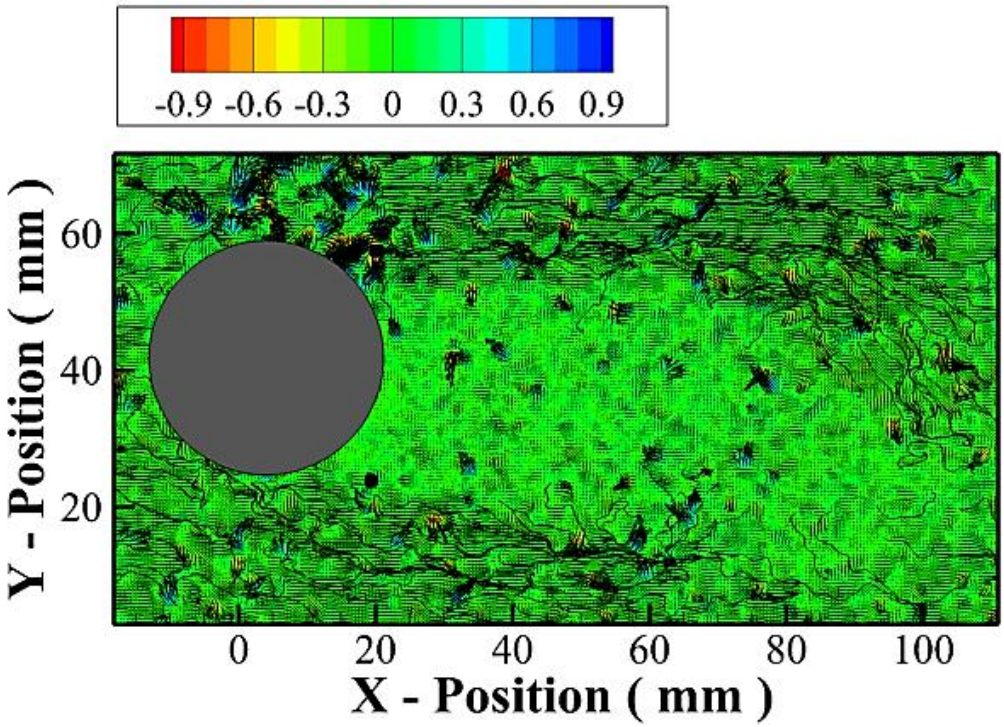

Figure 19. Downstream 20 mm pier, top view at 0.117 m / s speed.

It is shown in table 2 and table 3, downstream flow vortex and its position due to pier thickness for each corresponding speed. (500≤Re≤2000)

Pier (mm)	Y-Speed (m/s)	(Re)	X-Position (mm)
10	0.117	3289	6
20	0.117	3289	4
30	0.117	3289	1

Table 2. Vortex position in X at 0.117m/s speed.

Pier (mm)	Y-Speed (m/s)	(Re)	X-Position (mm)
10	0.163	4573	4
20	0.163	4573	2.5
30	0.163	4573	0

Table 3. Vortex position in X at 0.163 m/s speed.

The data from table 2 and table 3, is arranged to create a king of experimental nomogram shown in Figure 20, using at least two points water flow speed (Y-Speed (m/s)) and 10mm (blue line); 20 mm (red line) to 30mm (grey line) pier thickness for obtaining an horizontal vorticity distance (X-Position (mm)).

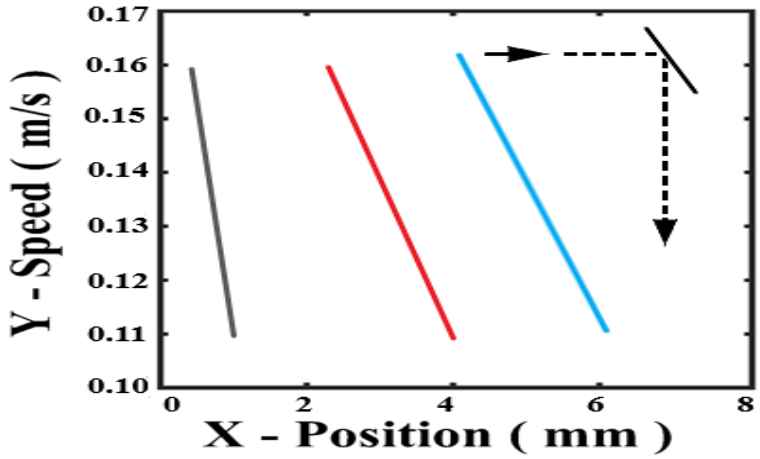

Figure 20. Horizontal vorticity distance nomogram, using speed and pier thickness.

(This work is licensed under a Creative Commons Attribution 4.0 International License.)

International Journal of Engineering Research & Technology (IJERT)
ISSN: 2278-0181
Vol. 9 Issue 03, March-2020

CONCLUSIONS

Using LaVision DaVis8 video software processing and post-processing with Tecplot 360 software, it was possible to obtain images of the study areas in two dimensions (flow profiles), in the upstream study area location, the flow through the slimmer pier, showed a linear trend behaviour, generating a moderate small vortex, and for next two piers, the flow tended to hit the bottom increasing its vorticity and going further back along distance at different positions. In the downstream study area location, the flow became increasingly abrupt as the pier thickness increased, observed by the number of vortices and vectors direction, until hitting against the pier. It is evident that the relationship is directly proportional, the bigger the thickness, the bigger the turbulence, and therefore a bigger scour probability. Analysis of variances for each pier indicates an important significant difference, but also from point of view of water flow visualisation at images, it is possible to see. Hence, the importance of building a slender pier as possible, where water flow passes by.

REFERENCES

[1] Adrian, R. J., "Scattering particle characteristics and their effect on pulsed laser measurements of fluid flow", speckle velocimetry vs particle image velocimetry, (1984), Appl. Optics 23, pp. 1690-91.
[2] Adrian, R. J., "Statistical properties of particle image velocimetry measurements in turbulent flow", Selected Papers 3rd Int. Symp. on Applications of Laser Anemometry to Fluid Mechanics ed T Asanuma et al (Lisbon: Ladoon), (1988), pp 115–290.
[3] Akoz, M. S., B. Sahin, and H. Akilli, "Flow characteristic of the horizontal cylinder placed on the plane boundary", Flow Measurement and Instrumentation, (2010), v. 21, p. 476-487.
[4] Bao, T., and Z. Liu, "Vibration-based bridge scour detection", A review: Structural Control and Health Monitoring, (2017), v. 24, p. n/a-n/a.
[5] Campa, A., F. Astorga, C. Alvarez, J. G. Murillo, and G. Estrada, "Enhanced Method of Particle Image Velocimetry Applied to Measure the Scour Phenomena in Bridge Piers", International Journal of Civil Engineering, (2016), (IJCE) ISSN(P): 2278-9987; ISSN(E): 2278-9995 Vol. 5, Issue 1.
[6] Hill, D. F., and B. D. Younkin, "PIV measurements of flow in and around scour holes", Experiments in Fluids, (2006), v. 41, p. 295-307.
[7] Keshavarzi, A., and J. Ball, "Enhancing PIV image and fractal descriptor for velocity and shear stresses propagation around a circular pier", Geoscience Frontiers, (2017), v. 8, p. 869-883.
[8] Martinez-Ramírez, J. D., and Fj Gonzalez. "Velocímetro de Particulas Basado En Imagenes Digitales." *Cenam.Mx*, (2015), pp. 1–5, https://www.cenam.mx/memsimp06/Trabajos Aceptados para CD/Posters/P-15.pdf.
[9] Moncada, M., T. Alix, P. Aguirre, P. Bolivar, C. Juan, N. Flores, and J. Edgar, "Estudio experimental sobre protección contra la socavación en pilas circulares", (2007), Revista Técnica, v. 30, p. 157.
[10] Oben-Nyarko, K., and R. Ettema, "Pier and Abutment Scour Interaction", Journal of Hydraulic Engineering, (2011), v. 137, p. 1598-1605.
[11] Radice, A., and V. Davari, "Roughening Elements as Abutment Scour Countermeasures", Journal of Hydraulic Engineering, (2014), v. 140, p. 6014014.
[12] Sturm, T. W, T. Stoesser, S. Hong, S. Kara, Wang, and Y. C., "Estimating Foundation Scour for Extreme Hydrologic Events at Scour-Critical Bridges", (2016), Report No.: FHWA- GARPXX.
[13] Willert, C. E., and M. Gharib, "Digital particle image velocimetry", (1991), Exp. Fluids 10, pp181-193.
[14] Younkin, B. D., "Prediction of scour formation due to a turbulent wall jet along a non-cohesive sediment bed", (2008), ProQuest Dissertations Publishing.

(This work is licensed under a Creative Commons Attribution 4.0 International License.)